KSME Journal, Vol. 9, No. 3, pp. 377~384, 1995

Flame Structure and Thermal NO_X Formation in Hydrogen Diffusion Flames with Reduced Kinetic Mechanisms

Su-Ryong Lee*, Sim-Soo Park* and Suk-Ho Chung**

(Received December 28, 1994)

Structure and thermal NO_X formation of hydrogen diffusion flames are studied numerically, by adopting a counterflow as a model problem. Detailed kinetic mechanism having twenty-one step hydrogen oxidation is systematically reduced to a two-step mechanism while five-step thermal NO_X chemistry of the extended Zel'dovich mechanism is reduced to one-step. Results show that the extinction strain rates are much higher than those for hydrocarbon flames and the NO_X production can be controlled by increasing strain rates which results in the decrease of flame temperature significantly. Comparison between the results of the detailed and reduced mechanisms demonstrates that the reduced mechanism successfully describes the essential features of hydrogen diffusion flames including the flame structure, extinction strain rate and NO_X production.

Key Words: Hydrogen, Diffusion Flame, Thermal NO_X, Extinction, Reduced Mechanism

1. Introduction

One-step overall reaction has been frequently adopted as a chemistry modeling in analyzing diffusion and premixed flames. As a result, only qualitative predictions can be made. For quantitative predictions, however, a set of multi-step elementary reactions should be accounted for. Recently, due to the advent of powerful computing capability, a detailed chemistry modeling of flame structure has been introduced. Methane/air diffusion flame structure was numerically studied by Dixon-Lewis et al.(1984) for the Tsuji burner geometry and the results are in good agreement with experiment. Dixon-Lewis and Missaghi(1988) analyzed the flame structure and extinction of hydrogen/air diffusion flames, and Pitz and Westbrook(1986) studied the autoignition of butane fuel in engine considering over 200 reaction steps.

Detailed chemistry modeling, however, is still impractical in applying to multi-dimensional or turbulent flames because of excessive computation time arising from many species involved in chemical reaction. Thus, reduced kinetic mechanisms have been developed by adopting proper steady-state approximations for reaction intermediaries and/or partial equilibrium assumptions for suitable reaction steps. Peters(1985) derived a four-step reduced kinetic mechanism for methane/air premixed flame and calculated the flame speed which was in good agreement with experiment. This four-step reduced mechanism has also been applied to the analysis of diffusion flame structure(Peters and Kee, 1987). The efforts to reduce the reaction steps are extended to the various kinds of fuels including the heavier hydrocarbon(Chung et al., 1993).

As a reduced kinetic mechanism predicts well the flame structure, matched asymptotic analyses have been performed to understand flame characteristics. Chung and Williams(1990) derived a two-step reduced mechanism for diffusion flames of CO/H_2 mixture as a model for a low calory fuel and analyzed the flame structure asymptotically. Lee and Chung(1994) analyzed the hydrogen diffusion flame asymptotically with

* Advanced Engineering and Research Institute, Hyundai Motor Co.

** Department of Mechanical Engineering, Seoul National University

two-step reduced mechanism.

These studies suggest that since the reduced mechanism depends on fuels, the application of a reduced mechanism should be developed for each fuel. Thus, the present study is focused on hydrogen fuel which is used as a liquid propellant and is considered to be a suitable fuel for a hypersonic flight. Due to the increasing awareness on environmental issues, hydrogen fuel is also considered as an alternative clean fuel for automotive use in the future. Thus, the objective of the present study is to analyze the flame structure and investigate the NO_x formation of hydrogen diffusion flames using reduced kinetic mechanism.

2. Formulation and Numerical Schemes

We consider a counterflow system, in which a nitrogen-diluted hydrogen jet impinges on a jet of air, and subsequently mixed stoichiometrically and reacted near the stagnation plane, having a planar diffusion flame stabilized. In a boundary layer approximation, counterflow system has a similarity solution by defining a stream function f and the mass flux V as

$$f'=\frac{u}{u_\infty},\quad V=\rho v \tag{1}$$

The transformed governing equations of continuity, momentum, species, energy, and mixture fraction are as follows:

$$\frac{dV}{dy}+(j+1)a\rho f'=0 \tag{2}$$

$$\frac{d}{dy}\left(\mu\frac{df'}{dy}\right)-V\frac{df'}{dy}+a[\rho_e-\rho(f')^2]=0 \tag{3}$$

$$-\frac{d}{dy}(\rho Y_i V_{iy})-V\frac{dY_i}{dy}+\omega_i W_i=0,\quad i=1,\ 2,\ \cdots,\ N \tag{4}$$

$$\frac{d}{dy}\left(\lambda\frac{dT}{dy}\right)-C_p V\frac{dT}{dy}-\sum_{i=1}^{N}\rho Y_i V_{iy}C_{pi}\times\frac{\partial T}{\partial y}-\sum_{i=1}^{N}\omega_i W_i h_i=0 \tag{5}$$

$$\frac{d}{dy}\left(\frac{\lambda}{C_p}\frac{dZ}{dy}\right)-V\frac{dZ}{dy}=0 \tag{6}$$

where T is the temperature, ρ the density, Y_i, W_i, and ω_i are the mass fraction, molecular weight, and reaction rate of i-th species, respectively, u and v the transverse and axial velocities, respectively, C_{pi} and h_i the specific heat and enthalpy of i-th species, respectively, C_p the specific heat of mixture, Z the mixture fraction, a the stretch factor defined in the free stream condition denoted by the subscript e, j the geometric factor for $j=0$ and 1 for two-dimensional and axisymmetric cases, respectively, and N the total number of species involved. V_{iy} is the diffusion velocity of i-th species in axial direction determined from the Curtis-Hirschfelder approximation and λ and μ the thermal conductivity and viscosity of a mixture determined from Wilke's formula. And the equation of state is

$$\rho=pW/RT \tag{7}$$

where p is the pressure, W the molecular weight of mixture, and R the gas constant.

These equations are subject to the following boundary conditions at the free stream.

$$y=-\infty:\ V=V_{-\infty},\ f'=\sqrt{\rho_\infty/\rho_{-\infty}},\ T=T_{-\infty},\ Y_i=Y_{i,-\infty},\ i=1,\ \cdots,\ N \tag{8}$$

$$y=\infty:\ f'=1,\ T=T_\infty,\ Y_i=Y_{i,\infty},\ i=1,\ \cdots,\ N \tag{9}$$

To account for the infinite boundary conditions at $\pm\infty$, the calculation domain is selected at $y=-L_F$ and $y=L_O$ which are sufficiently far from the boundary layer.

Thermodynamic properties and state equations are calculated from CHEMKIN(Kee et al., 1980) and transport properties from TRANSPORT package(Kee et al., 1983).

The starting mechanism is listed in Table 1 where the specific reaction rate constant k_k of the k-th reaction step is

$$k_k=B_k T^{\alpha_k}\exp(-E_k/RT). \tag{10}$$

The reaction rate of i-th species ω_i is the summation over all k-th steps involving i-th species. The mechanism contains 12 species and 21 reaction steps for H_2/O_2 reactions and 5 steps for thermal NO_x chemistry of the extended Zel'dovich mechanism corresponding to the steps $N1$ through $N5$.

Numerical calculation is based on Smooke's code(Smooke et al., 1986) by discretizing the governing equations into algebraic relations and

Table 1 Specific reaction-rate constants for starting mechanism of H_2-O_2-N_2 reaction system(Units : kJ/mol, mol/cm^3, s^{-1})

No.	Reaction	A_j	α_j	E_j
1	$H+O_2 \leftrightarrow {}^{b}OH+O$	2.0E14	0.0	70.30
2	$H_2+O \leftrightarrow OH+H$	5.06E4	2.67	26.30
3	$H_2+OH \leftrightarrow H_2O+H$	1.0E8	1.6	13.80
4	$OH+OH \leftrightarrow H_2O+O$	1.5E09	1.14	0.42
5[c]	$H+O_2+M \rightarrow {}^{c}HO_2+M$	2.3E18	−0.8	0.00
6	$H+HO_2 \rightarrow OH+OH$	1.5E14	0.0	4.20
7	$H+HO_2 \rightarrow H_2+O_2$	2.5E13	0.0	2.90
8	$OH+HO_2 \rightarrow H_2O+O_2$	6.0E13	0.0	0.00
9	$H+HO_2 \leftrightarrow O+H_2O$	3.0E13	0.0	7.20
10	$HO_2+O \leftrightarrow OH+O_2$	1.8E13	0.0	−1.70
11	$HO_2+HO_2 \rightarrow H_2O_2+O_2$	2.5E11	0.0	−5.20
12[a]	$OH+OH+M \leftrightarrow H_2O_2+M$	3.25E22	−2.0	0.00
13	$H_2O_2+H \leftrightarrow H_2O+OH$	1.0E13	0.0	15.00
14	$H_2O_2+OH \leftrightarrow H_2O+HO_2$	5.4E12	0.0	4.20
15[a]	$H+H+M \rightarrow H_2+M$	1.8E18	−1.0	0.00
16[a]	$H+OH+M \rightarrow H_2O+M$	2.2E22	−2.0	0.00
17[a]	$O+O+M \leftrightarrow O_2+M$	2.9E17	−1.0	0.00
18[a]	$H+O+M \leftrightarrow OH+M$	6.2E16	−0.6	0.00
19	$H_2O_2+H \leftrightarrow HO_2+H_2$	1.7E12	0.0	15.75
20[a]	$O+OH+M \leftrightarrow HO_2+M$	1.0E16	0.0	0.00
21	$H_2+O_2 \leftrightarrow OH+OH$	1.7E13	0.0	200.70
	Thermal NO_X mechanism			
N1	$O+N_2 \leftrightarrow N+NO$	1.9E14	0.0	319.03
N2	$N+O_2 \leftrightarrow O+NO$	1.129E10	1.0	27.83
N3	$N+OH \leftrightarrow NO+H$	4.795E13	0.0	5.23
N4	$NO+HO_2 \leftrightarrow NO_2+OH$	3.E12	0.5	10.08
N5	$NO+OH \leftrightarrow NO_2+H$	5.9E12	0.0	129.49

[a] Chaperon efficiences $H_2O/6.5/H_2/1.0,/O_2/0.4/N_2/0.4$

[b] Reversible reaction

[c] Forward reaction

solving it with Newton method and Euler time integration. Adaptive grid is employed since the reaction zone is very thin. The solution procedure is summarized in the following. For the grid point system M of

$$M=\{-L_F=y_0<y_1<\cdots<y_n=L_o\} \quad (11)$$

the finite differencing of the governing equations of Eqs. (2)~(6) leads to the following nonlinear algebraic equations.

$$F(U_k)=0 \quad (12)$$

where U_k is a dependent variable. To solve this, the following linear system is devised

$$J(U_k)(U_{k+1}-U_k)=-\lambda_k F(U_k),$$
$$k=1, \cdots, n-1 \quad (13)$$

which are to be solved by using iteration method, where $J(U_k)$ is the Jacobian matrix and λ_k the damping factor. Since factoring the matrix takes much time, we used the modified Newton method which determines the Jacobian periodically. Since the Newton method is sensitive to initial condi-

tions in convergence that the Euler time integration is also used to refine initial conditions.

3. Reduced Mechanism

Twenty-one steps of H_2-O_2 chemistry and five steps of nitrogen chemistry are adopted as a starting mechanism as is listed in Table 1. This starting mechanism can be reduced systematically as follows. Reaction rates of O, OH, HO_2 and H_2O_2 are orders of magnitude larger than the transport rates of these species and thus steady-state can be assumed for these species. This results in four algebraic equations which can be used to eliminate reaction steps of 2, 3, 7 and 12 in the balance equations for the remaining non-steady state species. Consequently, the starting mechanism is reduced to a two-step mechanism for hydrogen oxidation, given by

$$\text{I}: 3H_2+O_2 \leftrightarrow 2H_2O+2H \tag{14}$$

$$\text{II}: H+H+M \rightarrow H_2+M \tag{15}$$

which are hydrogen oxidation and radical generation(I) and radical recombination(II).

Preliminary numerical results indicate that the concentrations of N and NO are much lower than that of NO_2. Thus, one-step reduced NO_x mechanism can be derived from the extended Zel'dovich mechanism by using the steady-states for N and NO as

$$\text{III}: N_2+O_2 \leftrightarrow 2NO \tag{16}$$

The reaction rates of these reduced mechanisms are as follows.

$$\begin{aligned}\omega_I &= \omega_1+\omega_6+\omega_9+\omega_{11}-\omega_{14}-\omega_{17}-\omega_{19}\\ &\quad -\omega_{20}+\omega_{21}(-\omega_{N1}+\omega_{N2}-\omega_{N5})\\ \omega_{II} &= \omega_5-\omega_{11}+\omega_{13}+\omega_{14}+\omega_{15}+\omega_{16}\\ &\quad +\omega_{17}+\omega_{18}+\omega_{19}+\omega_{20}\\ \omega_{III} &= \omega_{N1}\end{aligned} \tag{17}$$

Here the terms in the parenthesis can be considered only in predicting NO_X formation. The overall flame structure including flame extinction is influenced little by neglecting these terms.

The steady-state approximations relate the concentrations of steady-state species with other species concentrations. Since these relations are algebraically complex, it is quite cumbersome to calculate the concentrations of the steady-state species and express them explicitly. Concentration of some steady-state species can be approximated from the corresponding partial equilibrium. Especially, the concentration of OH can be reasonably approximated from a partial equilibrium of step-3. This result can be fed into other steady-state relations to determine the concentrations such as O, HO_2 and H_2O_2. And then, the steady-state OH relation can be used for the refinement.

The partial equilibrium of step-3, i.e., $\omega_3 \approx 0$, dictates

$$[OH]=\frac{[H][H_2O]}{K_3[H_2]} \tag{18}$$

where K_k is the equilibrium constant of step-k. By neglecting the minor radicals of HO_2 and H_2O_2 in the steady-state relation for O, the concentration of O can be approximated as

$$[O]=\frac{\omega_{1f}+\omega_{2b}+\omega_{4f}}{k_{1b}[OH]+k_{2f}[H_2]+k_{4b}[H_2O]} \tag{19}$$

Then, the steady-states of HO_2 and H_2O_2 show the following relations.

$$\begin{aligned}[HO_2] &= (b_1^2/4+a_1)^{1/2}-b_1/2\\ a_1 &= \{\omega_5+\omega_{9b}+\omega_{10b}+\omega_{20f}+(Z_{14f}+Z_{19f})\\ &\quad \times(\omega_{12f}+\omega_{13b})\}/\{k_{11}(2-Z_{14f}-Z_{19f})\}\\ b_1 &= \{(k_6+k_7+k_{9f})[H]+k_8[OH]+k_{10f}[O]\\ &\quad +(k_{14b}[H_2O]+k_{19b}[H_2])(1-Z_{14f}\\ &\quad -Z_{19f})+k_{20b}[M]\}/\{k_{11}(2-Z_{14f}-Z_{19f})\}\\ Z_{14f} &= k_{14f}[OH]/(k_{12b}[M]+k_{13f}[H]\\ &\quad +k_{14f}[OH]+k_{19f}[H])\\ Z_{19f} &= k_{19f}[H]/(k_{12b}[M]+k_{13f}[H]\\ &\quad +k_{14f}[OH]+k_{19f}[H])\end{aligned} \tag{20}$$

$$[H_2O_2]=\frac{\omega_{11}+\omega_{12f}+\omega_{13b}+\omega_{14b}+\omega_{19b}}{k_{12b}[M]+k_{13f}[H]+k_{14f}[OH]+k_{19f}[H]} \tag{21}$$

For the refinement of O and OH concentrations, the steady-state relations of O and OH yield the following expressions.

$$\begin{aligned}[O] &= (b_2^2/4+a_2)^{1/2}-b_2/2\\ a_2 &= (\omega_{1f}+\omega_{2b}+\omega_{4f}+\omega_{9f}+\omega_{10b}\\ &\quad +2\omega_{17b}+\omega_{18b}+\omega_{20b})/2k_{17f}\\ b_2 &= \{(k_{1b}+k_{20f})[OH]+k_{2f}[H_2]\\ &\quad +k_{4b}[H_2O]+k_{9b}[H_2O]+k_{10f}[HO_2]\\ &\quad +k_{18f}[H]\}/2k_{17f}\end{aligned} \tag{22}$$

$$[OH]=(b_3^2/4+a_3)^{1/2}-b_3/2$$
$$a_3=(\omega_{1f}+\omega_{2f}+\omega_{3b}+2\omega_{4b}+2\omega_6+\omega_{10f}+2\omega_{12b}+\omega_{13f}+\omega_{14b}+\omega_{18f}+\omega_{20b}+2\omega_{21f})/2(k_{4f}+k_{12f}[M]+k_{21b})$$
$$b_3=\{(k_{1b}+k_{20f}[M])[O]+(k_{2b}+k_{16}[M])\times[H]+k_{3f}[H_2]+k_8[HO_2]+k_{13b}[H_2O]+k_{14f}[H_2O_2]+k_{18b}[M]+k_{10b}[O_2]\}/2(k_{4f}+k_{12f}[M]+k_{21b}) \quad (23)$$

Concentrations of N and NO are also determined from their respective steady-states as follows.

$$[N]=(\omega_{N1f}+\omega_{N2b}+\omega_{N3b})/(k_{N1b}[NO]+k_{N2f}[O_2]+k_{N3f}[OH]) \quad (24)$$
$$[NO_2]=(\omega_{N4f}+\omega_{N5f})/(k_{N4b}[OH]+k_{N5b}[H]) \quad (25)$$

4. Results and Discussions

Two-dimensional($j=0$) counterflow system is adopted as a model problem in the present study. Air is assumed a mixture of 79% N_2/21% O_2 and the fuel is hydrogen diluted with nitrogen. The pressure is 1 atm and the initial temperatures on both sides of fuel and air free streams are 298 K.

Figure 1 demonstrates the temperature and concentrations of major species as a function of mixture fraction for the free stream conditions of $a=2000\,s^{-1}$ and the hydrogen mole fraction on the fuel side of $X_{H_2,F}=0.8$. The solid lines are the results from starting mechanism and the dotted lines from reduced mechanism. The temperature and concentrations of major species agree well except the high temperature region where the results from the reduced mechanism slightly overpredict the temperature, O_2 and H_2O.

Radical profiles of O, OH and H are shown in Fig. 2. These profiles are in qualitative agreement, and the concentrations of O and OH are overpredicted in the reduced mechanism. On the other hand, better agreement for radical H can be seen since H is not assumed in steady-state. The reason of the overprediction of the temperature and species concentrations can be attributed to the steady-state approximations of radicals except H, such that the transport effect of diffusion and convection is not accounted for in the reduced mechanism, resulting in the overprediction.

Variations of the flame temperature with stretch are shown in Fig. 3. In general, flame temperature

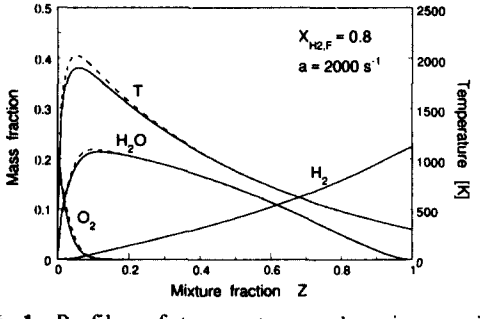

Fig. 1 Profiles of temperature and major species with mixture fraction for starting(solid line) and two-step reduced(dashed line) mechanisms

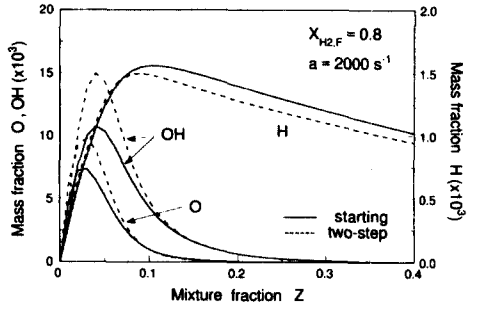

Fig. 2 Profiles of H, O and OH mass fractions with mixture fraction for starting and two-step reduced mechanisms

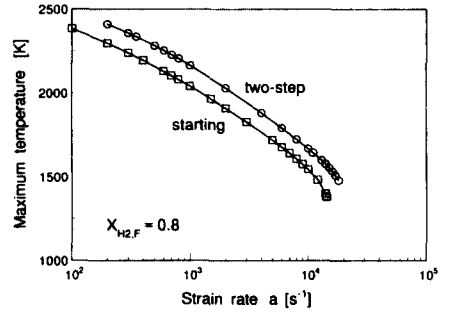

Fig. 3 Variations of maximum temperature as a function of strain rate for starting and two-step reduced mechanisms

should approach the adiabatic one when the stretch approaches zero if all the Lewis numbers are unity. This is because the characteristic flow time becomes long enough that the reaction reaches an equilibrium in the small stretch regime, that is, the reaction time is shorter than the fuel and oxidizer mixing time. As a result, the fuel and oxidizer at the reaction zone maintain low concentrations. As stretch is increased, due to the reduction in the characteristic flow time, chemical reaction can not be completed and leakages of fuel and oxidizer through the reaction zone increase, leading to the decrease in the flame temperature. As the stretch is further increased over $a=14300\,s^{-1}$, flame can not exist since the flow time becomes too short to sustain the flame.

The flame structure of hydrogen diffusion flame is quite different in nature, compared to that of hydrocarbon fuels such as methane. For methane, the flame structure in the reaction zone is composed of three zones ; the methane fuel consumption layer, water-gas shift reaction zone and oxidation layer of H_2 and CO. Even for the stretch near extinction for hydrocarbons, fuel leakage does not occur since the fuel is almost completely consumed in the fuel consumption layer, whereas significant amount of oxidizer leaks through the flame. However, for hydrogen flames, the fuel, i. e., hydrogen, leaks through the flame. This is demonstrated by the existence of the appreciable amount of hydrogen in the region between the flame and oxidizer boundary as can be seen in Fig. 1. This is partly because of the mass diffusivity and because the fuel to oxidizer mass ratio for stoichiometry are quite different between hydrogen and hydrocarbon fuels. The extinction strain rate for the present hydrogen fuel is an order of magnitude higher than that of hydrocarbon fuels, meaning that the hydrogen diffusion flame is difficult to extinguish.

For the entire range of the stretch, the prediction of flame temperature from the reduced mechanism is approximately 100 K higher than that from the starting mechanism. For $X_{H_2,F}=0.8$, the extinction strain rate a_E is $14300\,s^{-1}$ and $18000\,s^{-1}$ from the starting and reduced mechanisms, respectively.

The extinction strain rates as a function of nitrogen dilution are shown in Fig. 4, indicating that the extinction strain rate decreases with the dilution. The extinction strain rates agree well for the reduced and the starting mechanisms considering the variations with dilution. Thus the two-step reduced mechanism based on the approximation of steady-states of all the radicals except H can adequately represents the flame structure and the flame extinction.

Hydrogen fuel is considered as a clean fuel without generating such pollutants as unburnt hydrocarbon, carbon monoxide and soot. However, since the flame intensity of the hydrogen fuel is much stronger than hydrocarbon fuels, appreciable amount of nitrogen oxides are expected to be produced. To develope an efficient way of NO_x

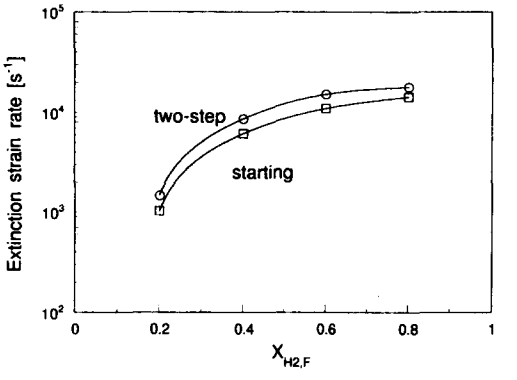

Fig. 4 Extinction strain rates as a function of fuel dilution for starting and two-step reduced mechanisms

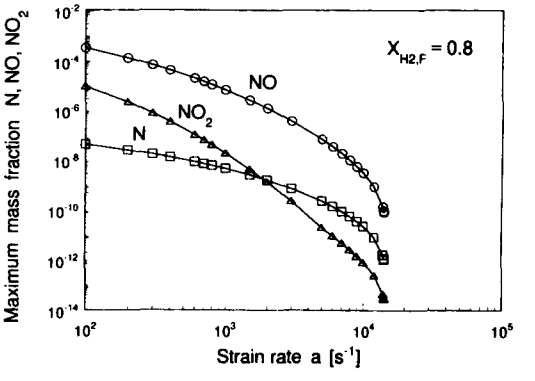

Fig. 5 Variations of N, NO and NO_2 as a function of strain rate for starting mechanism

control, understanding of the production of NO_X in hydrogen diffusion flames is essential.

Figure 5 shows the maximum mass fractions of N, NO and NO_2 as a function of strain rate for $X_{H_2,F}=0.8$ calculated from the starting mechanism. It demonstrates that the production of NO is several orders of magnitude greater than that of N and NO_2. This leads to the steady-state approximations for N and NO_2. The decrease in the production of NO_X, especially NO_2 is significant as the strain rate is increased, caused by the large activation energies associated with the thermal NO_X mechanism shown in Table 1. As the strain rate is increased, the flame temperature decreases, thereby the nitrogen oxides production is greatly reduced. Since the flame can be sustained up to very high strain rate for hydrogen flames, the production of nitrogen oxides can be lower than that from hydrocarbon fuels, because the flame temperature of hydrogen at high strain rate is about several hundred degrees lower than that of hydrocarbon. Since the strain rate in the present study can be related to a scalar dissipation rate for turbulent diffusion flames, method of increasing turbulence in a combustor could be a measure of reducing nitrogen oxides for hydrogen diffusion flames.

As an indication of NO_X production in turbulent diffusion flames, Peters and Donnerhack(1981) proposed the integration of NO_X production rate divided by density over the mixture fraction as

$$I_{NO,t}=\int_0^t \frac{\omega_{NO,t}(Z)}{\rho(Z)}dZ. \tag{26}$$

Figure 6 demonstrates the integral of I_{NO} as a function of stretch for various dilution in fuel hydrogen. Since I_{NO_2} is approximately two orders lower than I_{NO}, only I_{NO} is plotted. The results indicate that NO_X formation is greatly reduced by increasing stretch. Comparison of the reduced one-step NO_X mechanism with the starting mechanism shows that the prediction from the reduced mechanism is somewhat higher, again due to the overprediction of the flame temperature. Considering NO_X production with stretch which covers several orders, the prediction with one-step

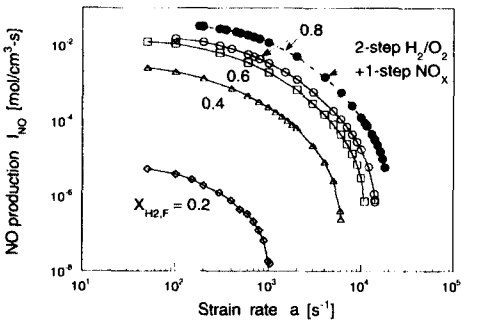

Fig. 6 Comparison of NO_X production as a function of strain rate(open symbol ; starting mechanism, closed symbol ; reduced mechanism)

NO_X mechanism is satisfactory. This indicates the potential applicability of the reduced mechanism for both the flame structure and the formation of thermal NO_X.

5. Concluding Remarks

The structure and thermal NO_X formation of hydrogen diffusion flame with stretch including flame extinction conditions have been analyzed numerically for both the starting mechanism and the reduced mechanism of two-step H_2/O_2 and one-step NO_X mechanisms. The agreement between these results are satisfactory.

For the hydrogen diffusion flames, the extinction stretch is much higher and the flame can survive at much lower flame temperature than hydrocarbon flames. The flame temperature and extinction characteristics can be quantitatively predicted from the two-step reduced H_2-O_2 reactions and the NO_X production can be predicted with the one-step NO_X mechanism, based on the assumption of the steady-state of all the radicals except H and NO.

Major source of the NO_X is from NO, because NO_2 production can be negligible for hydrogen diffusion flames. This characteristics is different from the thermal NO_X production for the methane/ethane mixture fuel where the NO and NO_2 productions are comparable(Chung et al., 1993). As a possible NO_X reduction, hydrogen diffusion flame can be burnt at very high turbulence intensity flow field, thereby reducing flame tempera-

ture and NO production while maintaining stable combustion since the flame is difficult to extinguish.

Acknowledgment

This work has been supported by the Korea Science and Engineering Foundation through Turbo and Power Machinery Research Center and by the Hyundai Motor Company.

References

Chung, S. H. and Williams, F. A., 1990, "Asymptotic Structure and Extinction of CO/H_2 Diffusion Flames with Reduced Kinetic Mechanisms," *Combustion and Flame*, Vol. 82, pp. 389~410.

Chung, S. H., Lee, S. R., Mauss, F. and Peters, N., 1993, "Reduced Kinetic Mechanisms and NO_X-Formation in Diffusion Flames of CH_4/C_2H_6 Mixtures," in *Reduced Kinetic Mechanisms for Applications in Combustion Systems*(Eds. Peters, N. and Rogg, B.), Springer-Verlag, pp. 308~328.

Dixon-Lewis, G., David, T., Gaskell, P. H., Fukutani, S., Jinno, H., Miller, J. A., Kee, R. J., Smooke, M. D., Peters, N., Effelsberg, E., Warnatz, J. and Behrendt, F., 1984, "Calculation of the Structure and Extinction Limit of a Methane-Air Counterflow Diffusion Flame in the Forward Stagnation Region of a Porous Cylinder," *Twentieth Symposium (International) on Combustion*, The Combustion Institute, Pittsburgh, pp. 1893~1904.

Dixon-Lewis, G. and Missaghi, M., 1988, "Structure and Extinction Limits of Counterflow Diffusion Flames of Hydrogen-Nitrogen Mixtures in Air," *Twenty-second Symposium* (International) on Combustion, The Combustion Institute, pp. 1461~1470.

Kee, R. J., Miller, J. A. and Jefferson, T. H., 1980, "CHEMKIN : A General-Purpose, Problem-independent, Transportable, Fortran Chemical Kinetics Code Package," Sandia National Laboratories Report, SAND80-8003.

Kee, R. J., Warnatz, J. and Miller, J. A., 1983, "A Fortran Computer Code Package for the Evaluation of Gas-phase Viscosities, Conductivities, and Diffusion Coefficients," Sandia National Laboratories Report, SAND 83-8209.

Lee, S. R. and Chung, S. H., 1994, "On the Structure of Hydrogen Diffusion Flames with Reduced Kinetic Mechanisms," *Combust. Sci Tech.*, Vol. 96, pp. 247~277.

Pitz, W. J. and Westbrook, C. K., 1983, "Chemical Kinetics of the High Pressure Oxidation of n-Butane and Its Relation to Engine Knock," *Combustion and Flame*, Vol. 63, pp. 113~133.

Peters, N., 1985, *Numerical Simulation of Combustion Phenomena*(Glowinski, R., Larroutarou, B. and Teman, R. Eds.), Lecture Notes in Physics 241, Springer-Verlag, pp. 90~109.

Peters, N. and Donnerhack, S., 1981, "Structure and Similarity of Nitric Oxide Production in Turbulent Diffusion Flames," *Eighteenth Symposium (International) on Combustion*, The Combustion Institute, pp. 33~42.

Peters, N. and Kee, R. J., 1987, "The Computation of Stretched Laminar Methane-Air Diffusion Flames Using a Reduced Four-Step Mechanism," *Combustion and Flame*, Vol. 68, pp. 17~29.

Smooke, M. D., Puri, I. K. and Seshadri, K., 1986, "A Comparison between Numerical Calculations and Experimental Measurements of the Structure of a Counterflow Diffusion Flame Burning Diluted Methane in Diluted Air," *Twenty-first Symposium(International) on Combustion*, The Combustion Institute, Pittsburgh, pp. 1783~1792.